One-step synthesis of dimethyl ether from syngas with Fe-modified zeolite ZSM-5 as dehydration catalyst

Jianchao Xia[1,2], Dongsen Mao[2,*], Bin Zhang[2], Qingling Chen[2] and Yi Tang[1]

[1]*Department of Chemistry and Shanghai Key Laboratory of Molecular Catalysis and Innovative Materials, Fudan University, Shanghai 200433, P. R. China*

[2]*Shanghai Research Institute of Petrochemical Technology, SINOPEC, Shanghai 201208, P. R. China*

Received 20 July 2004; accepted 09 September 2004

A number of Fe-containing ZSM-5 zeolites, such as HFeZSM-5 and HFeAlZSM-5 prepared by hydrothermal synthesis and Fe-modified ZSM-5 through solid-state ion-exchange, were adopted as methanol dehydration catalysts for syngas to dimethyl ether (STD) process. Their structures, acidic and basic properties were characterized by XRD, ESR, ICP-AES, TPD and FT-IR. Among these Fe-containing zeolites, the Fe-modified ZSM-5 displayed the highest dimethyl ether selectivity, least CO_2 production. Some correlations between catalytic performance and acidity and basicity of Fe-containing ZSM-5 zeolite were discussed.

KEY WORDS: Fe-containing ZSM-5 zeolites, methanol, dehydration, dimethyl ether, syngas, acidity, basicity, modification.

1. Introduction

Dimethyl ether (DME) has received a world-wide attention as a clean alternative fuel for diesel engines since it was disclosed to have better combustion performance than the conventional diesel fuel, e.g. lower NO_x emission, lesser smoke and engine noise [1]. Recent analyses have also revealed the approach to apply DME as an economical alternative to LPG.

The conventional process of DME production, called two-step method, has become more and more insufficient with the growing demand for DME as fuels for these new applications. Lately, an original technique named STD (synthesis gas to dimethyl ether) process was developed for the direct synthesis of DME from synthesis gas in a single reactor on hybrid catalysts composed of copper-based methanol synthesis catalysts and solid acids [2, 3]. The key steps in the STD process are methanol synthesis, methanol dehydration and the water gas shift reaction (WGSR):

$$2CO + 4H_2 = 2CH_3OH \qquad \Delta H = -180.58\,\text{kJ/mol} \tag{1}$$

$$2CH_3OH = CH_3OCH_3 + H_2O \qquad \Delta H = -23.41\,\text{kJ/mol} \tag{2}$$

$$H_2O + CO = H_2 + CO_2 \qquad \Delta H = -40.96\,\text{kJ/mol} \tag{3}$$

The combination of these reactions results in a synergistic effect relieving the unfavourable thermodynamics for methanol synthesis: methanol, product in the first step, is consumed for reaction to dimethyl ether and water. The water is shifted by the WGSR reaction (3) forming carbon dioxide and hydrogen, the latter being a reactant for the methanol synthesis. Thus, one of the products of each step is a reactant for another. This creates a strong driving force for the overall reaction allowing very high syngas conversion in one single pass.

The most common hybrid catalysts reported in the literature for STD process are the physical mixture of the methanol synthesis catalyst and the solid acid catalyst. A lot of solid acids such as γ-Al_2O_3 [4, 5], silica-alumina [4, 6], TiO_2–ZrO_2 [4, 7], and zeolites [4–6, 8–11] were used as dehydration catalysts for DME synthesis. Xu *et al.* [4] reported that HZSM-5 was the most active among the catalysts tested. However, it is well known that the strong acidic sites on HZSM-5 zeolites promote the generation of secondary products like hydrocarbons [4, 6]. Furthermore, Joo *et al.* [12] reported recently that the strong acid sites of solid acid catalysts deteriorate the selectivity to DME by the water reforming reaction of methanol and DME producing carbon dioxide and hydrogen. Hence, the modification of HZSM-5 is a key step to improve the selectivity for DME synthesis.

In this paper, a number of Fe-containing ZSM-5 zeolites prepared by different methods were, for the first time, adopted as a methanol dehydration catalyst in the STD process. Good catalytic performance was achieved by Fe-modified ZSM-5 zeolites. Structures, acidities and basicities of these Fe-containing ZSM-5 zeolites were characterized by XRD, ESR, ICP-AES, TPD and FT-IR and were related to the catalytic properties.

* To whom correspondence should be addressed.
E-mail: maods@sript.com.cn; yitang@fudan.edu.cn

1011-372X/04/1200–0235/0 © 2004 Plenum Publishing Corporation

2. Experimental

2.1. Preparation of Fe-containing ZSM-5 zeolites

Fe-containing ZSM-5 zeolites were prepared by using two different methods including hydrothermal synthesis (HTS) and solid-state ion-exchanging (SSIE). In the HTS process, 1.01 $\sim$ 2.02 g $Fe(NO_3)_3 \cdot 9H_2O$, without or with 0.77 g $Al(NO_3)_3 \cdot 9H_2O$, was dissolved in 21.90 g of deionized water to form solution A. After adding 1.2 g sodium hydroxide, the 24.40 g aqueous solution of TPAOH (25 wt% TPAOH) was mixed with 22.50 g silica sol (40 wt% SiO_2) to form solution B. Being homogeneous, the solution A was slowly added into solution B in 2 min under stirring and aged for half an hour. The mixed solution was then transferred to a Teflon lined autoclave and heated to 443 K for 2 days. The synthesized product was white and turned to be buffy after a template removing step treating in air at 823 K for 4 h. To obtain H-form of FeZSM-5, the product was ion exchanged three times with 1 M ammonium nitrate solution at 353 K for 1 h and finally calcined in flowing air at 823 K for 4 h. The obtained samples were named as HFe-30 (Si/Fe = 30), HFe-60 (Si/Fe = 60) and HFeAl-60 (Si/Al = 60, Si/Fe = 60).

In the SSIE process, 10 g HZSM-5 with a molar ratio of Si/Al equal to 30 (named HAl-30) was mechanically mixed with 1.01 or 2.02 g $Fe(NO_3)_3 \cdot 9H_2O$ in a ball mill for 1 h. The resulting mixture was calcined at 823 K for 4 h in the presence of air. The obtained zeolites were designated as HFeAl-S1 and HFeAl-S2, respectively.

2.2. Catalyst characterization

X-Ray diffraction analysis was performed on a Rigaku D/MAX-1400 diffractometer with a Cu target, a voltage of 40 kV and a current of 40 mA. The data of surface area and pore volume were collected through nitrogen gas adsorption on Micrometric TriStar 3000 instrument.

Elemental analysis of potassium exchanged FeZSM-5 was carried out by ICP-AES method. Before element analysis the Na-form FeZSM-5 was mixed with a 1 M potassium nitrate solution and stirred at 353 K for 24 h. The amount of potassium in solution was greatly superfluous for the exchanging of sodium. Electron spin resonance (ESR) spectra were recorded on ER200D-SRC (Brucker) at SF = 9.74 GHz, MA = 5 G, MF = 100 kHz and CF = 3050 G.

FT-IR spectra at 673 K and room temperature were measured with an IFS88 IR spectrometer (Brucker). The zeolite/KBr wafers were pretreated in a vacuum (1.33×10^{-2} Pa) at 673 K for 2 h, and then introduced to record the IR spectra in hydroxyl region at 673 K. IR spectra at room temperature were collected till the wafers cooled down under the same vacuum.

The strength and distribution of acidity of these Fe-containing ZSM-5 zeolites were determined by temperature-programmed-desorption of ammonia (NH_3-TPD). About 0.10 g of the pelletized samples was activated in the reactor at 823 K in a flow of helium gas for 40 min. After cooling to room temperature, ammonia gas was injected in the reactor to assure saturated absorption on the samples. The physisorbed ammonia was desorbed by a flow of helium gas at 423 K for about 1 h. The strength distribution of acidity was obtained through NH_3-TPD from 423 to 823 K in a flow of helium gas. The CO_2-TPD was applied to examine the basicity of Fe-containing zeolite in a procedure similar to NH_3-TPD.

2.3. Reaction studies

$Cu/ZnO/Al_2O_3$ (an industrial methanol synthesis catalyst, Cu/Zn/Al = 60:30:10 atomic ratio) was used as the methanol synthesis catalyst. The Fe-containing ZSM-5 samples were mechanically mixed with the $Cu/ZnO/Al_2O_3$ before use as catalysts for STD process. The weight ratio of Fe-containing ZSM-5 and $Cu/ZnO/Al_2O_3$ was at 1:2. The combined catalysts were prereduced by a premixed gas (5% H_2 in N_2) at 513 K for 6 h. Then, catalytic test was carried out in a fixed-bed reactor at 4 MPa, and at 533 K, with a GHSV (gas hourly space velocity) of synthesis gas at 1500 $cm^3/(g_{cat} \cdot h)$. The effluent was analyzed by an on-line chromatograph (HP 4890D) after the system was stabilized for 3–4 hours. TCD and FID detectors were used to examine the inorganic and organic products, respectively.

3. Results and discussion

3.1. Catalytic properties

Table 1 listed the data of catalytic test of the admixed catalysts using different Fe-containing zeolites as methanol dehydration components under the same conditions. It can be seen that very high CO conversion (about 94%) was achieved with all the ZSM-5 containing catalysts except HFe-30 and HFeAl-S2. More methanol (about two times), detected in the products of HFe-30, showed the lower activity on dehydration of methanol, which should be responsible for the lower CO conversion on HFe-30 than over other solid acids. The even lower conversion of CO (ca. 73%) with a lower methanol selectivity on HFeAl-S2 should be ascribed to a reason different from the one of low dehydration activity of HFe-30.

Profitably, compared to HAl-30, apparent decrease in CO_2 production was observed on all of the Fe-containing solid acids, indicating that Fe-treatment was a promising method in enhancing the DME selectivity of ZSM-5 in STD process. Especially, the CO_2 selectivity decreased by about 20%, resulting in a corresponding increase in DME selectivity on the admixed catalyst using HFeAl-S1 as the dehydration catalyst.

Table 1
Effect of dehydration components on catalytic properties of admixed catalyst in the STD process

Dehydration components	Conversion of CO (%)	Selectivity (%)			
		DME	CO_2	Methanol	Hydrocarbons
HFe-60	94.09	54.90	41.60	3.44	0.06
HFe-30	83.42	52.66	40.84	6.37	0.13
HFeAl-60	94.52	57.66	38.95	3.36	0.03
HAl-30	93.10	48.22	49.06	2.67	0.05
HFeAl-S1	95.49	67.06	29.63	3.28	0.03
HFeAl-S2	73.44	59.39	37.44	3.03	0.14

Reaction conditions: $P = 4$ MPa, $T = 533$ K, GHSV $= 1500\ cm^3/(h \cdot g_{cat})$, $H_2/CO = 2$.

Table 2
Surface area and pore volume of FeZSM-5 zeolites

Sample	S_{BET} (m^2/g)	Pore volume (cm^3 /g)	Average pore diameter (nm)
HAl-30	380.51	0.2630	2.76
HFe-30	363.17	0.2889	3.18
HFe-60	383.33	0.2508	2.64
HFeAl-60	388.36	0.3401	3.50

Nevertheless, the increasing amount of Fe in HFeAl-S2 displayed undesirable effects on the catalytic properties, causing the generation of hydrocarbons and more CO_2.

3.2. Characterization of the Fe-containing ZSM-5 zeolites

3.2.1. Structural properties

Surface area and pore volume of hydrothermally synthesized samples were listed in table 2. All the samples had a similar surface-area at about 380 m^2/g except HFe-30, which had a little lower value ($\sim 363\ m^2/g$) mainly due to the large amount of extraframework iron formed in strong basic medium [13]. The large surface areas would indicate well-developed pore structure of the Fe-containing zeolites and ZSM-5 zeolite for the post-synthesis treatment with ferric nitrate. Moreover, the sample HFeAl-60, containing aluminum as well as ferric ions, has especially larger pore volume and bigger pore diameter than those zeolites that only contain aluminum or ferric ions. All the samples were well crystallized as testified by the XRD results in figure 1.

Ferric oxide tetrahedron in the framework (FW) of zeolites contains one negative charge just as aluminum oxide tetrahedron and need one extraframework (EFW) positive charge carrier for compensation. So the moles of potassium ions in potassium-exchanged samples can be expected to equal with the moles of FW ferric ions, and the molar ratio of K/Fe can be accordingly used to indicate the ratio of Fe_{FW}/Fe_{total} when no other framework substitution in the framework [13]. In our study about 59% ferric ions in sample HFe-60 entered the zeolitic framework and a little less (at about 40%) in

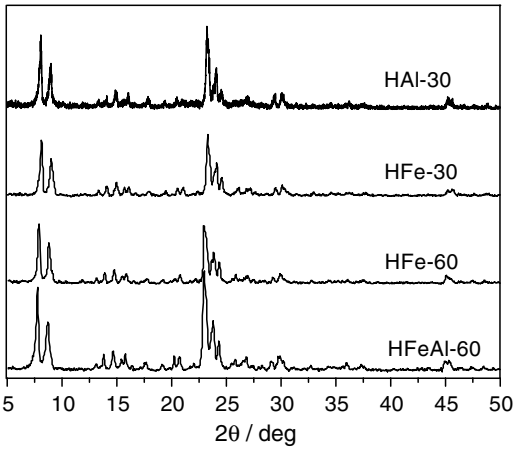

Figure 1. XRD patterns of ZSM-5 type zeolites prepared by hydrothermal synthesis.

Table 3
Content of iron and potassium of potassium-exchanged Fe-ZSM zeolites

Sample	Fe (wt %)	K (wt %)	Mol ratio of K/Fe
HFe-30	3.31	0.93	0.40
HFe-60	1.81	0.74	0.59

sample HFe-30 according to the results of ICP-AES (see table 3) when the crystallization was carried out in strong basic medium. The results validated the large amount of EFW Fe ions in sample HFe-30 and naturally agreed with the data of surface area in table 2.

ESR spectroscopy has been used to identify the states of chemical combination of Fe-containing zeolites by many authors [14–17]. When the symmetry is spherical (such as in perfect tetrahedral or octahedral symmetries), the signal would be observed at $g = 2.0023$ (figure 2). The signal at $g = 4.3$ of figure 2(a) indicated the presence of ferric ions in lattice position of MFI in distorted tetrahedral symmetry [13]. Curve (b) displayed weaker ESR signal at $g = 4.3$, which make it clear that only few ferric ions were incorporated into the lattice of zeolites by solid-state ion-exchange method.

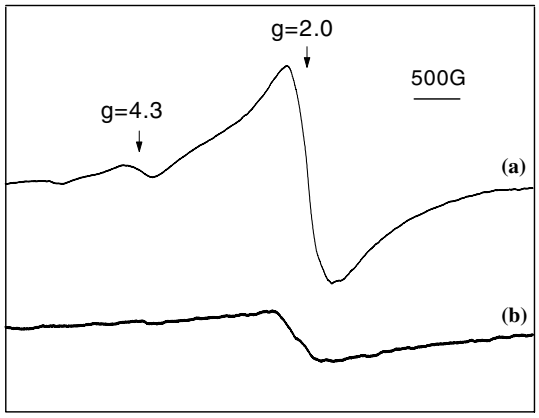

Figure 2. ESR spectra of (a) HFe-60 and (b) HFeAl-S1.

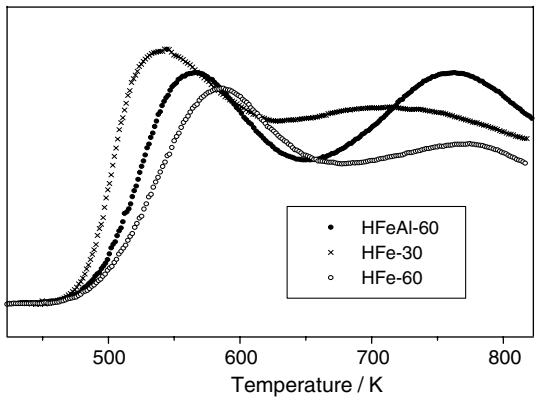

Figure 3. TPD curves for ammonia in H-form Fe-containing ZSM-5 zeolite prepared by hydrothermal synthesis.

3.2.2. Acidic and basic properties

NH_3-TPD curves (see figures 3 and 4) of all the Fe-containg ZSM-5 samples revealed two kinds of acidic sites occurring on the surface of these zeolites. One of them is the weaker acidic site that appeared a peak at the lower temperature of about 550 K and the other is the stronger one with the peak of TPD curve at a higher temperature of about 750 K. Of all the hydrothermal synthesized Fe-containing samples HFeAl-60 possessed the largest amount of strong acid sites (figure 3) because of the existence of Al(OH)Si groups, acidity of which is stronger than that of Fe(OH)Si groups [18]. A weak peak and a much weaker peak at high temperature were observed on the TPD curves of HFe-60 and HFe-30, respectively, disclosing very small concentration of strong acidic sites on the two samples.

The amount of weak acidic sites decreased in the sequence: HFe-30 > HFeAl-60 > HFe-60. Nevertheless, the strength of weak acidic sites fell in the reverse order: HFe-60 > HFeAl-60 > HFe-30. Sample HFe-30 had the largest amount of weak acidic sites mainly because of its abundant EFW ferric ions. And the least ferric and aluminous ions in sample HFe-60 resulted in the smallest amount of weak acidic sites. The lowest strength of weak acidic sites on HFe-30 was also related to the large amount of EFW ferric ions, which can engender weak acidic sites in the form of Fe_nOH just as Al_nOH groups but much weaker than Al_nOH groups. HFeAl-60 bore the lower strength of weak acidic sites than HFe-60 not only because of the larger amount of ferric and aluminous ions but also of the extra EFW Fe ions produced by the competition between Fe and Al on incorporating into the lattice of zeolites as it is well known that it is much easier for Al ions to enter into the framework of zeolites than for Fe ions.

Figure 4 depicted the acidic properties of Fe-treated and untreated H-ZSM-5 zeolites. The TPD curves of treated samples took on less area of peak at high temperature and possessed a shift of low-temperature peak to lower temperature. Hereby, we can conclude that Fe-incorporation decreases the number of strong

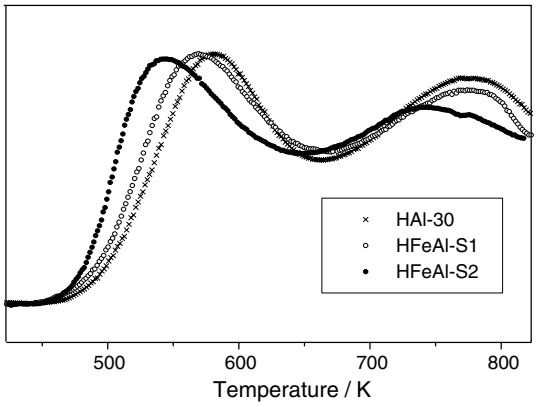

Figure 4. TPD curves for ammonia in ZSM-5 zeolites before and after modification by ferric nitrate.

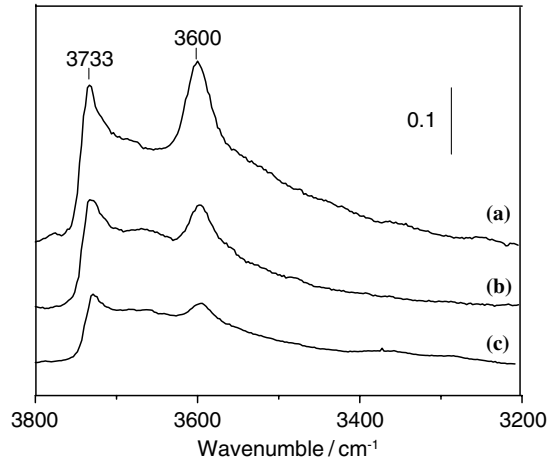

Figure 5. Infrared spectra in the hydroxyl region of (a) HAl-30 (b) HFeAl-S1 and (c) HFeAl-S2 at 673 K.

acid sites and engenders many new weaker acidic sites than the weak acidic sites on HAl-30. The decreased concentration of strong acid sites were also validated by the weakened IR bands at 3733 and 3600 cm^{-1} in figure 5 (due to terminal silanols and bridging hydroxyl

groups, respectively) after the treatment of ferric nitrate under calcination. The new weak acidic sites were probably from the loaded ferric ions and the EFW "alumina" ions brought from the lattice of zeolite by the post-treatment. The signal at $g = 2.0023$ of figure 2(b) displayed the evident existence of EFW ferric ions. Moreover, the weakened bands in figure 5 at 3600 cm^{-1} showed that the FW Al decreased during the procedure of Fe application, from which we can conclude that a great deal of "alumina" ions had transferred from framework to extraframework positions.

The same results were revealed by the IR spectra at room temperature in figure 6. An absorbance at 3665 cm^{-1}, assigned to hydroxyl groups on EFW Al, increased with the increase of ferric ions loaded, indicating that dealuminization occurred during the post-treatment with ferric nitrate. Differently, a shift of about 10 cm^{-1} to higher wavenumbers was observed on the IR spectra at room temperature compared with the spectra at 673 K because of the weakening effects of low temperature on the strength of H–O bonds. The bands at 3733 and 3600 cm^{-1} in figure 5, respectively, moved to 3742 and 3616 cm^{-1} in figure 6. The sharp band at 3702 cm^{-1}, observed in the sample HAl-30, can be attributed to the υ(OH) band of free OH groups of water species adsorbed on the Brønsted acid sites as reported by Wakabayashi *et al.* [19]. In addition, the broad band at 3565 cm^{-1} may be assigned to the vibrations of hydrogen-bonded silanols or hydroxyl groups on Brønsted acid sites although any unquestionable explanation has not been brought forward [19, 20]. This broad band disappeared on the spectra of HFeAl-S1 and shifted to 3589 cm^{-1} on the spectra of HFeAl-S2.

The dehydration of methanol is considered to occur on the acid sites of catalysts. The relationship between acidic properties and catalytic performance of solid acids for methanol dehydration has been studied by many researchers. It has been reported that the acid sites of weak or intermediate strength are responsible for selective formation of DME [4, 6, 12], while the strong acid sites may accelerate the formation of by-products such as CO_2 [12] and hydrocarbons [4, 6], which causes the DME selectivity to decrease. On the other hand, Kim *et al.* [8] reported recently that the strong acid sites of HZSM-5 zeolites are responsible for the formation of DME, while the acid sites appearing below 450 °C in the NH_3-TPD spectra are not important for dehydration of methanol to DME.

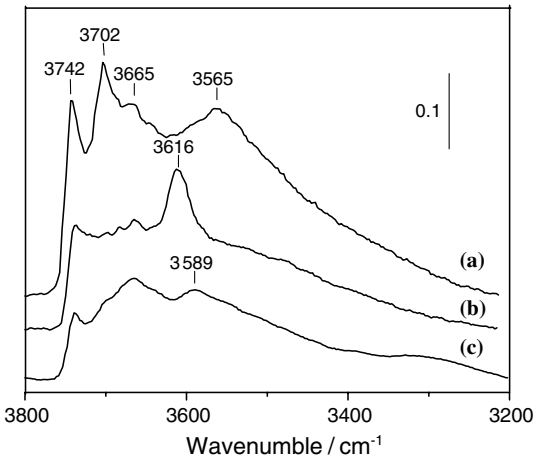

Figure 6. Infrared spectra in the hydroxyl region of (a) HAl-30 (b) HFeAl-S1 and (c) HFeAl-S2 at room temperature.

In the present paper, the highest methanol selectivity of HFe-30 among the three hydrothermally synthesized samples can be ascribed to its weakest acid strength (figure 3). The higher methanol selectivity on HFe-30 when compared to HFe-60 was due to the weaker acid sites than those present on HFe-60 even though their concentrations were larger. The lower methanol dehydration rate limited the conversion of the produced methanol to DME, resulting in the lower DME selectivity and lower CO conversion. On the other hand, the high activity of HFe-60 and HFeAl-60 samples for methanol dehydration resulted in high DME selectivity, and high CO conversion in spite of the difference in acid strength. These results indicated that when the acidity of solid acid was strong enough, the catalytic activity of the combined catalyst rested on the activity of the methanol synthesis component. On the other hand, when the acidity was not strong enough the catalytic activity was determined by dehydration ability of solid acid. Same conclusion had been drawn recently by Kim *et al.* [8].

As to the HAl-30 and Fe-modified HFeAl-S1 and HFeAl-S2 samples, high methanol dehydration activity was achieved due to the presence of strong acid sites, leading to similar methanol selectivity (ca. 3%). However, their CO_2 selectivity was very different, resulting in obvious difference in DME selectivity. Joo *et al.* [12] suggested that CO_2 was formed by water reforming reaction of methanol catalyzed by strong acid sites. After the formation of methanol, the acid catalyst catalyzed both dehydration to form DME and water reforming reaction to form CO_2. The decrease in strong acid sites decreased the reforming reaction, and it increased the selectivity of the dehydration reaction. However, in the present work, we think that the decrease in strong acid sites on HFeAl-S1 compared to HAl-30 was so small that it could not decrease the formation of CO_2 so much (ca. 20% decrease in CO_2 selectivity). On the other hand, the decrease in strong acid sites on HFeAl-S2 was greater than that on HFeAl-S1, but the decrease in CO_2 selectivity on HFeAl-S2 was smaller than that on HFeAl-S1. This result suggests that some other sites on HZSM-5 zeolites should be responsible for the formation of CO_2.

Since methanol is synthesized on basic catalysts and decomposition of methanol is the reverse of methanol synthesis [21, 22], methanol can be decomposed by the basic sites on HZSM-5 zeolites. Accordingly, the basicities of HAl-30 before and after Fe-modification were

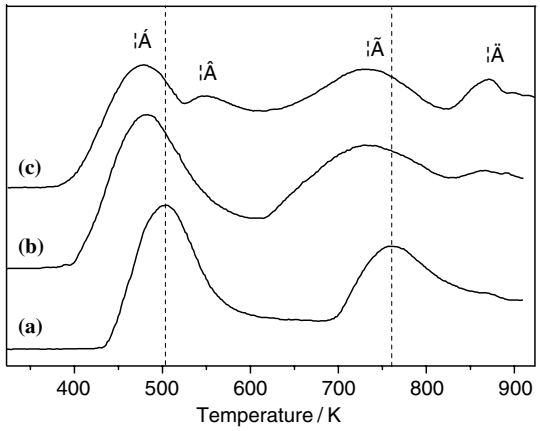

Figure 7. CO_2-TPD curves of (a) HAl-30 (b) HFeAl-S1 and (c) HFeAl-S2.

measured by CO_2-TPD method. As shown in figure 7, two peaks were observed in all the three samples, one of which at about 500 K (α) and the other at about 750 K (γ). After Fe modification, both peaks α and γ shifted to lower temperatures, indicating the decrease in the strength of basic sites, which led to the decrease of CO_2 production from methanol decomposition on basic sites. So the CO_2 production on HFeAl-S1 was much lower than that on HAl-30. However, two new peaks β and δ were found on HFeAl-S2 (figure 7C). The peak δ, at about 870 K, represented stronger basicity than other peaks and should be responsible for the larger amount of CO_2 and CH_4 by-products on HFeAl-S2 than on HFeAl-S1. Recently, Wu *et al*. [23] also found that CO, CO_2 and CH_4 was produced from the decomposition of methanol catalyzed by basic sites on SAPO-34.

4. Conclusions

Different methods were applied to prepare Fe-containing ZSM-5 zeolites. 40% and 59% Fe ions were separately incorporated into the framework of zeolites when ratios of Si/Fe were at 30 and 60 through hydrothermal synthesis in strong basic medium. Few ferric ions entered the lattice through post-treatment of HZSM-5 with ferric nitrate. All the Fe-modified zeolites possessed weaker acidity than HZSM-5.

Some delectable results were obtained in the catalytic test using these solid acids as methanol dehydration catalysts in the STD process. Catalytic activities remained unchanged when some amount of ferric ions were loaded, but decreased with an increase of the amount of ferric ions in sample HFe-30 and HFeAl-S2. The amount of CO_2 decreased for each Fe-containing zeolite and especially for HFeAl-S1, which was prepared by solid-state ion-exchange procedure. The main reason for less CO_2 production was that the basicity of HZSM-5 zeolite was weakened by Fe-modification.

Acknowledgment

The authors appreciated the financial supports from National Basic Research Program of China (No. 2003CB615801).

References

[1] J.B. Hansen and T. Oishi, Petrotech. 20 (1997) 823.
[2] K. Fujimoto, K. Asami, T. Shikada and H. Tominaga, Chem. Lett. (1984) 2051.
[3] D.M. Brown, B.L. Bhatt, T.H. Hsiung, J.J. Lewnard and F.J. Waller, Catal. Today 8 (1991) 279.
[4] M. Xu, J.H. Lunsford, D.W. Goodman and A. Bhattacharyya, Appl. Catal. A 149 (1997) 289.
[5] Q. Ge, Y. Huang, F. Qiu and S. Li, Appl. Catal. A 167 (1998) 23.
[6] T. Takegchi, K. Yanagisawa, T. Inui and M. Inoue, Appl. Catal. A 192 (2000) 201.
[7] V. Vishwanathan, H.S. Roh, J.W. Kim and K.W. Jun, Catal. Lett. 96 (2004) 23.
[8] J.H. Kim, M.J. Park, S.J. Kim, O.S. Joo and K.D. Jung, Appl. Catal. A 264 (2004) 37.
[9] Q. Ge, Y. Huang and F. Qiu, React. Kinet. Catal. Lett. 63 (1998) 137.
[10] G. Qi, J. Fei, X. Zheng and Z. Hou, Catal. Lett. 72 (2001) 121.
[11] K. Sun, W. Lu, F. Qiu, S. Liu and X. Xu, Appl. Catal. A 252 (2003) 243.
[12] O.S. Joo, K.D. Jung and S.H. Han, Bull. Korean Chem. Soc. 23 (2002) 1103.
[13] P. Ratnasamy and R. Kumar, Catal. Today 9 (1991) 329.
[14] L.M. Kustov, V.B. Kazansky and P. Ratnasamy, Zeolites 7 (1987) 79.
[15] G.P. Handreck and T.D. Smith, J. Chem. Soc. Faraday Trans. I. 85 (1989) 319.
[16] R.Q. Long and R.T. Yang, Catal. Lett. 74 (2001) 201.
[17] P. Fejes, I. Kiricsi, K. Làzár, I. Marsi, A. Rockenbauer, L. Korecz, J.B. Nagy, R. Aiello and F. Testa, Appl. Catal. A 242 (2003) 247.
[18] C. Chu and C. Chang, J. Phys. Chem. 89 (1985) 1569.
[19] F. Wakabayashi, J.N. Kondo, K. Domen and C. Hirose, Catal. Lett. 38 (1996) 15.
[20] M.B. Sayed, R.A. Kydd and R.P. Cooney, J. Catal. 88 (1984) 137.
[21] K.C. Waugh, Catal. Today 15 (1992) 51.
[22] X.R. Zhang, P. Shi, J. Zhao, M. Zhao and C. Liu, Fuel Proc. Tech. 83 (2003) 183.
[23] X. Wu, M.G. Abraha and R.G. Anthony, Appl. Catal. A 260 (2004) 63.